EFFECTS OF HIGH ENERGY BALL MILLING ON THE PROPERTIES OF COAL FLY ASH

A. Shaaroni, P.J. Liew*, R. Izamshah, J.M.Juoi

Fakulti Teknologi dan Kejuteraan Industri dan Pembuatan,
Universiti Teknikal Malaysia Melaka, Hang Tuah Jaya,
76100 Durian Tunggal, Melaka, Malaysia

*Coresponding Author's Email: payjun@utem.edu.my

ABSTRACT: Fly ash (FA), a byproduct of coal combustion, is produced in large quantities primarily by thermal power plants worldwide. Various methods have been employed to safely dispose of FA while adding value to it. To prevent pollution caused by the direct disposal of FA, it has been modified and utilized in other applications for its beneficial properties. One such modification method is high-energy ball milling, which refines the particle dimensions of FA by repeatedly applying stress and energy, thereby altering its physical and chemical characteristics. This process significantly reduces the particle size of FA, enhancing its fineness, reactivity, and surface area, making it suitable for various applications. In this study, high-energy wet ball milling was used to refine FA particles. Samples were collected from the ball-milled FA at regular intervals over an 8-hour milling process, and various characterization techniques were used to analyse their properties. X-ray diffraction was used to measure the crystallite size, and a particle size analyzer was employed to determine the particle size of the ball-milled FA. Field Electron Scanning Electron Microscopy (FESEM) was used to examine the microstructure of the particles. The results indicated that after the milling process, the spherical shape of the FA transformed into an irregular shape, and the average particle size was reduced from 20 μm to 1.5 μm.

KEYWORDS: *Fly ash; ball mill; particle size; x-ray diffraction*

1.0 INTRODUCTION

Fly ash (FA) is a byproduct of burning pulverized coal in thermal power plants, consisting of fine particles carried up with the exhaust gases. This residue is captured by electrostatic precipitators or other particle filtration equipment before being released into the atmosphere [1]. FA consists of inorganic, non-combustible materials present in coal, which fuse into a glassy, amorphous form during combustion [2]. Generally, FA particles are round, alkaline, and grey in appearance. Micro-sized particles of silicon dioxide (SiO_2), aluminum oxide (Al_2O_3), and calcium oxide (CaO) are typically found in fly ash [3].

FA is categorized into two classes, Class F and Class C, based on the volume of SiO_2, Al_2O_3 and iron oxide (Fe_2O) present. Class F FA, also known as pozzolanic FA, is extracted from the combustion of bituminous or anthracite coal. To be classified as Class F, SiO_2, Al_2O_3, and Fe_2O_3 must constitute more than 70% of the total composition. Class C FA resulting from the combustion of lignite or sub-bituminous coal, is both pozzolanic and cementitious. For Class C, SiO_2, Al_2O_3, and Fe_2O_3 must make up more than 50% of the total composition [4-5].

However, disposing of fly ash presents several major challenges. These include the creation of large wastelands, the significant water required for draining into wetlands, and the potential health and environmental risks from heavy metal leaching and airborne ash [6]. Consequently, extensive research has focused on effectively utilizing FA to mitigate the potential negative impacts of landfilling, brick production, concrete manufacturing, various civil engineering applications, and heat transfer applications on the environment and human health [7-9].

In an effort to add value to FA, it was subjected to high-energy ball milling. This process results in finer particles with increased surface area, enhanced reactivity, and potential modifications in chemical composition and thermal behaviour [10]. These characteristics make high-energy

ball-milled FA a promising material for advanced applications in construction, environmental remediation, and energy storage.

Ball milling has been crucial process in the ceramic processing and powder metallurgy industries for a long time, aiming to reduce particle size, mix or blend materials, and alter particle shapes [11]. The effectiveness of particle size reduction in ball milling depends on the chosen parameters. According to Pohshna et al. [12], the ball-to-powder ratio, milling vial volume, milling duration, and milling speed are the parameters most sensitive to particle size, with milling speed being the most critical.

For instance, Bakri et al. [13] achieved an average particle size of 60 nm from 10 μm after 6 hours of high-speed milling at 600 rpm using a high-energy planetary ball mill. In contrast, Li et al. [14] could only reduce the average particle size of FA from 36 μm to 2 μm after 96 hours of milling at a lower speed of 93 rpm. However, in another study, Li et al. [15] used a high-energy pulverization ball mill at 700 rpm and managed to reduce the average particle size of FA from 5 μm to 300 nm after nearly 67 hours. Meanwhile, Paul et al. [16] using a high-energy pulverization wet milling method with toluene as the medium at 300 rpm for 60 hours, successfully reduced the FA size from 60 μm to 148 nm. Hamada et al. [17] confirmed the superiority of wet milling over dry milling. Their analysis clearly showed that wet milling is a better method for reducing FA particle size, producing a much finer particle size distribution than dry milling.

Patil et al. [18] investigated the effects of planetary ball milling parameters on the mechano-chemical activation of FA by comparing three types of medium and surfactant, and by modifying the ball-to-powder ratio in the wet milling method. They found that Triton TX-100 (4 wt% in ethanol medium) with a 12:1 ball-to-powder ratio was the most effective in reducing particle size compared to cetyltrimethylammonium bromide (CTAB) and sodium lauryl sulfate (SLS). Meanwhile, in ethyl acetate medium, SLS showed better results. The 12:1 ball-to-powder ratio also yielded the best results compared to ratios of 8:1 and 10:1, indicating that ball-to-powder ratio is crucial in ball milling as it can reduce the milling time. Kanti et al. [19] used a 20:1 ball-to-powder ratio and reduced FA size from 5 μm to 55.5 nm after 30 hours, even at a speed of 300 rpm. In contrast, other researchers using a 10:1 ball-to-powder ratio only managed to reduce the size from 92 nm to 29 nm in the same amount of time [20]. This demonstrates the significant impact of the ball-to-powder ratio on the efficiency of particle size reduction during the ball milling process.

Despite advancements in the field, research on high-speed wet milling and its effects on FA particle properties remains limited. Therefore, this study aims to address this gap by investigating how adjustments in high-energy ball milling impact the microstructure and physical properties of FA. This integrated approach not only explores the relationship between milling parameters and FA properties but also aims to make significant contributions to the field of material science, particularly in the area of particle processing and characterization.

2.0 METHODOLOGY

2.1 Sample Preparation

Fly ash (FA) was obtained from the Jimah Power Plant in Port Dickson, Malaysia. The fresh FA was initially sieved using a 20 μm sieve, as the particles were relatively large, with an average size ranging from 100 to 300 μm. The sieved FA was then subjected to ball milling for further refining.

2.2. High Energy Ball Milling

Reduction in particle size of the FA was achieved using a high-energy planetary ball mill (Retsch EMAX) under wet milling conditions at a speed of 1200 rpm. The specific milling conditions are detailed in Table 1. SLS was added as a surfactant to prevent agglomeration of the ceramic particles in FA. Samples were taken out at 2-hour intervals and dried in an oven at 80 ºC for 8 hours to assess their characteristics.

Table 1: Ball Mill parameter conditions

Medium	Toulene
Surfactants	SLS at ration 100:1
Jar	50 ml zirconia jar
Ball	1 mm zirconia ball
Ball to powder ration	10:1
Time	8 hours rest for 5 min at 2-hour interval

2.3 Characterization of FA

The elemental composition of sieved fresh FA was determined using an X-ray fluorescence (XRF) spectrometer (Shimadzu 720). Energy Dispersive X-ray Spectroscopy was used to determine the elements in fresh FA. X-ray diffraction (XRD) studies were also conducted using CuKα radiation (λ = 1.54056 Å) at an accelerating voltage of 30 kV and a current of 20 mA to determine the crystallite size of the quartz phases in both fresh and ball-milled fly ashes. The samples were scanned over a 2θ range of 10 to 90°. A Field Electron Scanning Electron Microscope (FESEM) was used to evaluate the morphology of sieved fresh FA and ball-milled FA. To ensure conductivity, the FA samples were sputtered with gold using an auto fine coater sputtering unit. Images were captured at suitable accelerating voltages to achieve the best possible resolution using secondary electron imaging. The particle size distribution was measured using a Malvern Mastersizer Hydro 2000MU & Scirocco 2000 particle analyser. This equipment can measure sample sizes ranging from 0.02 μm to 2000 μm using automation software.

3.0 RESULTS AND DISCUSSIONS

3.1 XRF Analysis

Table 2 shows the material composition of FA, which obtained using the XRF analysis. As can be seen from Table 2, the main elements are SiO_2 (63.5%), Fe_2O_3 (17.06%), Cao (6%) and Al_2O_3 (5.2%), with the remaining composition consisting of other elements. This FA can be classified as Class F, as the total composition of SiO_2, Fe_2O_3, and Al_2O_3 is 85.76%, exceeding the 70% requirement for this classification.

Table 2: Material composition of FA (%) obtained through XRF analysis

SiO_2	Fe_2O_3	CaO	Al_2O_3	K_2O	SO_3	BaO	OTHER ELEMENTS
63.50	17.06	6.00	5.20	2.64	2.43	1.09	2.08

3.2 EDX Analysis

Figure 1 displays the FESEM image of the area selected for EDX analysis, while Figure 2 presents the typical EDX results of fresh FA. Table 3 lists the elements identified in the selected area. The analysis indicates that the fresh FA sample primarily comprises of oxygen (O), followed by silicon (Si), iron (Fe), calcium (Ca), and a small amount of aluminum (Al).

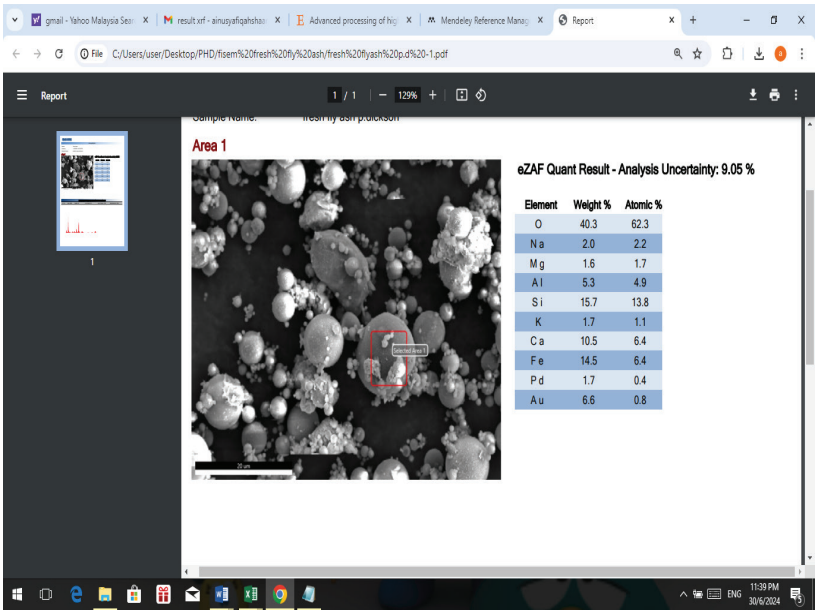

Figure 1: Area selected for EDX analysis in sieved fresh FA

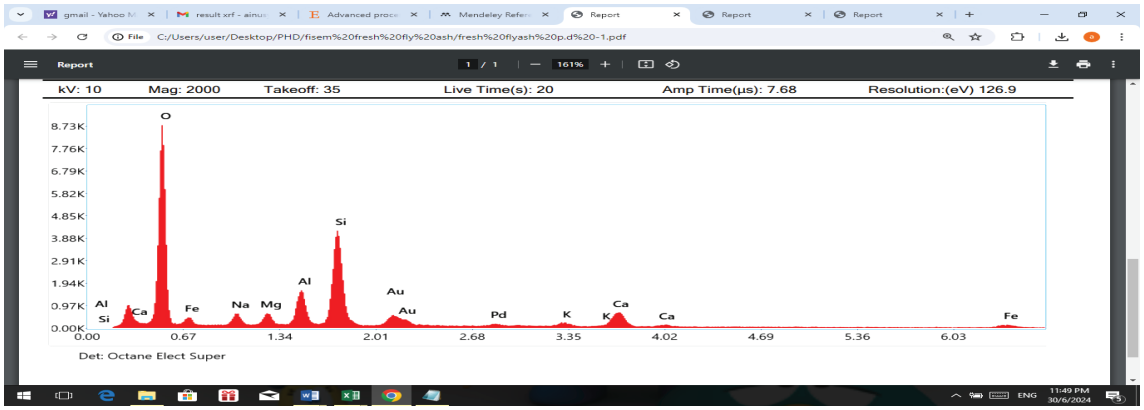

Figure 2: EDX result of sieved fresh FA

Table 3: EDX result at certain area of fly ash

Element	Weight%	Atomic%
O	40.3	62.3
Na	2	2.2
Mg	1.6	1.7
Al	5.3	4.9
Si	15.7	13.8
K	1.7	1.1
Ca	10.5	6.4
FE	14.5	6.4
Pd	1.7	0.4
Au	6.6	0.8

3.3 X-Ray Diffraction Analysis

X-ray diffraction (XRD) analysis was performed on the FA samples to identify their mineral composition. The XRD analysis revealed several crystalline peaks, including quartz, mullite, and hematite, as shown in Figure 3. A reduction in the number of peaks was observed in the ball-milled FA samples compared to the fresh fly ash, indicating significant material size reduction over the milling durations of 2 hours, 4 hours, 6 hours, and 8 hours. Specifically,

quartz (SiO_2) exhibited peaks at 26.33°, 26.49°, 26.35°, 26.36°, and 26.42° at 2θ values, highlighting changes in crystalline structure and particle size resulting from the ball milling process.

From Figure 3, it is evident that as the milling duration increases, the peak intensity of the quartz phase decreases, and the peaks become broader. Ball-milled FA shows a reduced degree of crystallinity, although several crystalline peaks are still visible in the diffractogram. This suggests that while mechanical milling reduces crystallinity, some crystalline phases remain detectable.

The average crystallite size was calculated using Scherrer's equation, which correlates the full width at half maximum (FWHM) of the X-ray diffraction peak with the crystallite size [21].

$$D = \frac{k\lambda}{\beta cos\theta} \quad (1)$$

Where;
D = particle diameter
λ = X-Ray wavelength
β = FWHM of the diffraction peak
θ = diffraction angle
k = Scherrer's constant

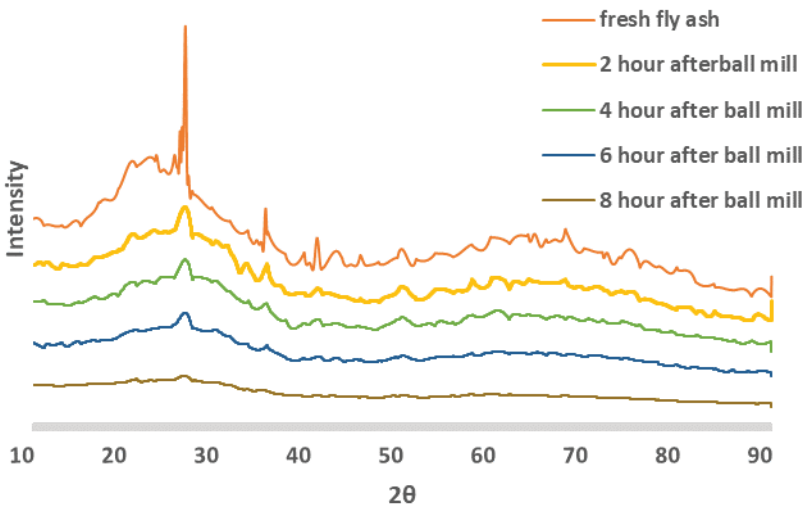

Figure 3: XRD pattern of fresh FA and after ball milled

3.4 Morphology Studies

The FESEM micrographs of fresh FA and samples after 2, 4, 6, and 8 hours of ball milling are depicted in Figure 4. Initially, the fresh FA particles were observed to be spherical with a smooth textured surface. These dense particles are known as cenospheres, contrasting with hollow spheres or plerospheres [21]. However, after ball milling, it was observed that the shape of the FA particles became coarser and irregular, consistent with observations reported by Bakri et al. [13]. However, after 6 and 8 hours of ball milling, the FA particles started to agglomerate, as depicted in Figure 4(d) and Figure 4(e).

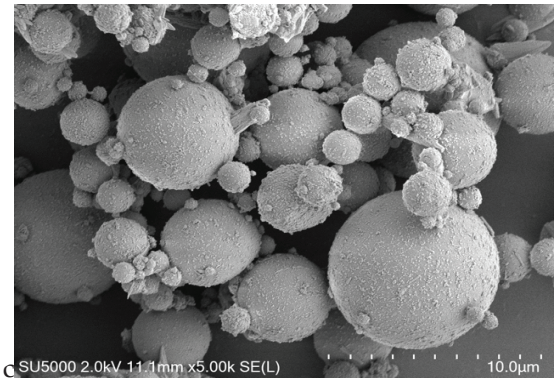

(a) Fresh FA

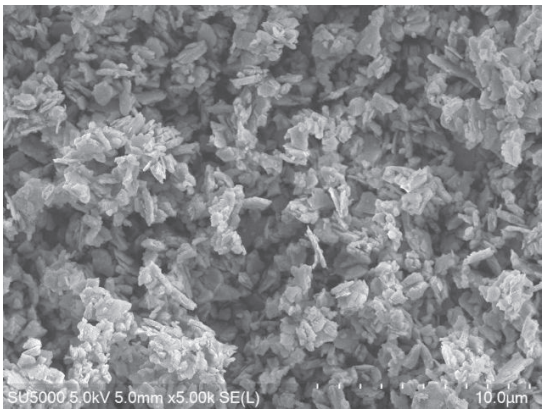

(b) 2 hours ball-milled FA

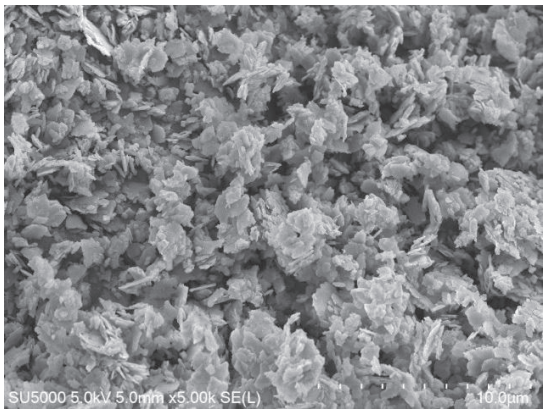

(c) 4 hours ball-milled FA

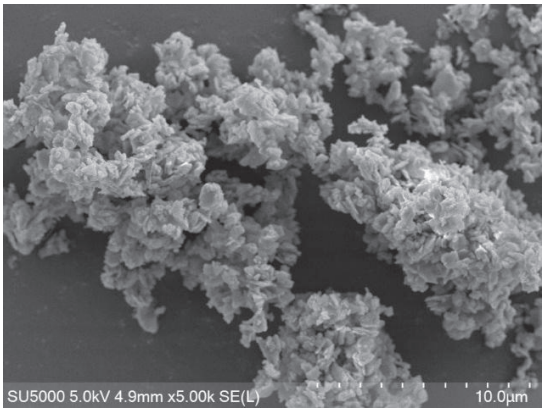

(d) 6 hours ball-milled FA

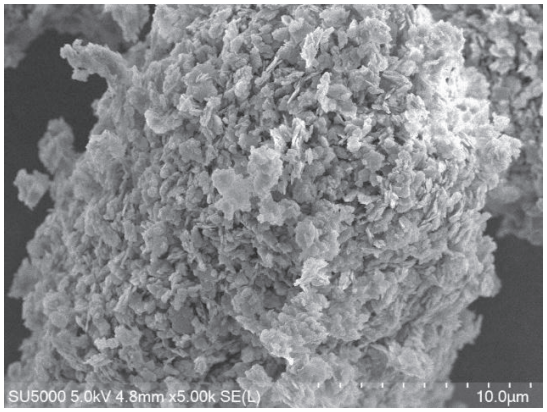

(e) 8 hours ball-milled FA

Figure 4: FESEM images of FA

3.5. Particle Size Analysis

An analysis of the size distribution during the milling process (Figure 5) reveals several intriguing observations. Initially, the fresh FA had particle sizes up to 300 µm. To expedite and minimize the ball milling duration, the sample was sieved using a 20 µm sieve. As depicted in Figure 5, the size distribution rapidly shifted leftward (towards smaller particle sizes) within the first 2 hours of milling. However, after 6 hours, particles in the range of 25 µm were also observed, indicating potential agglomeration of FA particles. By the end of 8 hours of milling, particles larger than 10 µm had largely disappeared, forming a new peak with a median size of approximately 1.5 µm.

This outcome is achieved because high-energy ball milling is a mechanical process that reduces particle sizes to nanometers using milling equipment with substantial kinetic energy. The process involves applying high mechanical loads to the milling vessel, which leads to frequent collisions, abrasion, and deformation that effectively decrease particle size [22].

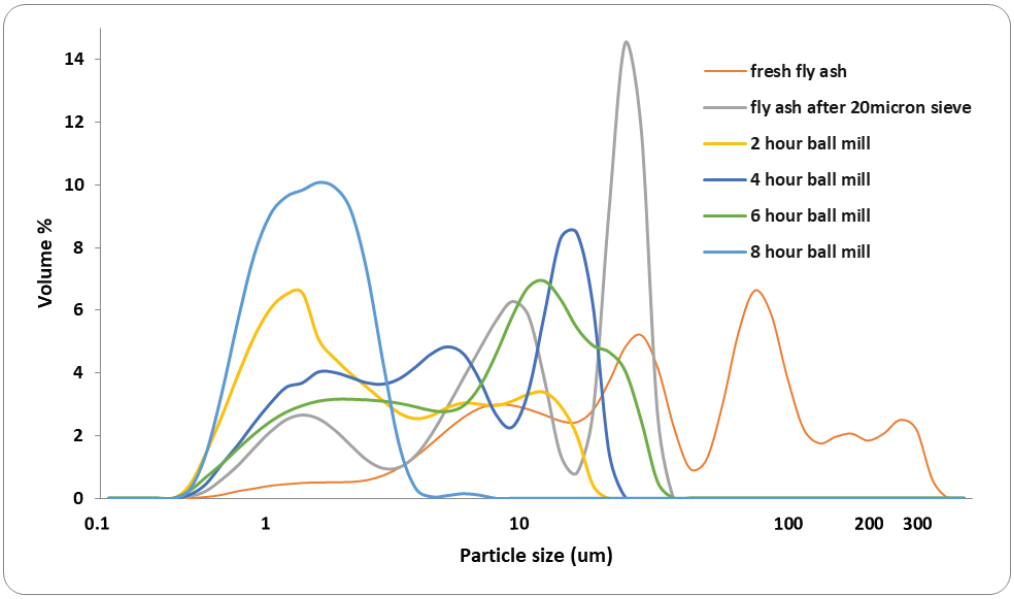

Figure 5: Particle size distribution

4.0 CONCLUSIONS

The research findings on FA characteristics after ball milling yield several significant conclusions. Ball milling significantly altered the physical properties of FA, including its crystallinity, morphology, and overall structure, transitioning it from a spherical to an irregular shape. Furthermore, ball milling effectively reduced FA particle size, demonstrating a decrease from 20 μm to an average of approximately 1.5 μm after 8 hours of processing.

Understanding these changes holds practical implications for enhancing the utilization of FA in applications where material performance and sustainability improvements are desired. In conclusion, ball milling emerges as an effective technique to modify the properties of FA thereby opening new opportunities for its utilization across various industries and applications. Future research could further explore additional parameters or combinations to optimize these modifications for specific uses.

ACKNOWLEDGMENTS

This study is funded by Ministry of Higher Education (MOHE) of Malaysia through the Fundamental Research Grant Scheme (FRGS), No: FRGS/1/2023/TK10/UTEM/02/6. The authors also would like to thank Universiti Teknikal Malaysia Melaka (UTeM) for all the support.

REFERENCES

[1] K. Maqsood, "Multiobjective optimization of thermophysical properties of indonesian fly-ash nanofluid," *Materials Today: Proceedings*, vol. 49, pp. 1255–1262, Jan. 2022, doi: 10.1016/J.MATPR.2021.06.304.

[2] P. Kanti, K. v. Sharma, C. G. Ramachandra, and B. Panitapu, "Stability and thermophysical properties of fly ash nanofluid for heat transfer applications," *Heat Transfer*, vol. 49, no. 8, pp. 4722–4737, Dec. 2020, doi: 10.1002/htj.21849.

[3] C. S. Reddy, S. Mohanty, and R. Shaik, "Physical, chemical and geotechnical characterization of fly ash, bottom ash and municipal solid waste from Telangana State in India," *International Journal of Geo-Engineering*, vol. 9, no. 1, Dec. 2018, doi: 10.1186/s40703-018-0093-z.

[4] ASTM C618-19, "Standard Specification for Coal Fly Ash and Raw or Calcined Natural Pozzolan for Use in Concrete," ASTM International. 2019.

[5] S. S. Alterary and N. H. Marei, "Fly ash properties, characterization, and applications: A review," *Journal of King Saud University - Science*, vol. 33, no. 6, p. 101536, Sep. 2021, doi: 10.1016/J.JKSUS.2021.101536.

[6] M. Ambrus and G. Mucsi, "Advanced processing of high Ca fly ash for enhanced reactivity and improved high value-added application possibilities," *Case Studies in Construction Materials*, vol. 18, p. e02214, Jul. 2023, doi: 10.1016/J.CSCM.2023.E02214.

[7] P. Jun Liew, H. Seng Tay, C. Yee Yap, I. Sharhida Othman, and R. Izamshah Raja Abdullah Fakulti Kejuruteraan Pembuatan, "Tribological behaviour of palm oil mixed with fly ash microparticles as a bio-based lubricant for manufacturing processes," 2021.

[8] L. Miao, M. Wen, C. Jiao, S. He, and X. Guan, "Concrete microstructure characterized by multi-measurement techniques considering fly ash contents and concrete sample sizes," *Case Studies in Construction Materials*, vol. 20, p. e03315, Jul. 2024, doi: 10.1016/J.CSCM.2024.E03315.

[9] Z. Liu, J. Han, and L. Hu, "Mechanical properties and microstructure of cement-fly ash-dacite powder composite cementitious system," *Developments in the Built Environment*, vol. 17, p. 100305, Mar. 2024, doi: 10.1016/J.DIBE.2023.100305.

[10] B. Peng *et al.*, "Preparation of mullite whiskers from high alumina fly ash and its reinforced porous structure," *Journal of Materials Research and Technology*, vol. 24, pp. 3323–3333, May 2023, doi: 10.1016/j.jmrt.2023.03.219.

[11] C. C. Koch, "The synthesis and structure of nanocrystalline materials produced by mechanical attrition: A review," *Nanostructured Materials*, vol. 2, no. 2, pp. 109–129, Mar. 1993, doi: 10.1016/0965-9773(93)90016-5.

[12] C. Pohshna and D. R. Mailapalli, "Modeling the particle size of nanomaterials synthesized in a planetary ball mill," *OpenNano*, vol. 14, p. 100191, Nov. 2023, doi: 10.1016/J.ONANO.2023.100191.

[13] A. M. M. al Bakri, H. Kamarudin, M. Bnhussain, J. Liyana, and C. M. Ruzaidi, "Nano geopolymer for sustainable concrete using fly ash synthesized by high energy ball milling," in *Applied Mechanics and Materials*, 2013, pp. 169–173. doi: 10.4028/www.scientific.net/AMM.313-314.169.

[14] M. G. Li, C. J. Sun, S. H. Gau, and C. J. Chuang, "Effects of wet ball milling on lead stabilization and particle size variation in municipal solid waste incinerator fly ash," *Journal of Hazardous Materials*, vol. 174, no. 1–3, pp. 586–591, Feb. 2010, doi: 10.1016/j.jhazmat.2009.09.092.

[15] H. Li, Y. Chen, Y. Cao, G. Liu, and B. Li, "Comparative study on the characteristics of ball-milled coal fly ash," *Journal of Thermal Analysis and Calorimetry*, vol. 124, no. 2, pp. 839–846, May 2016, doi: 10.1007/s10973-015-5160-5.

[16] K. T. Paul, S. K. Satpathy, I. Manna, K. K. Chakraborty, and G. B. Nando, "Preparation and characterization of nano structured materials from fly ash: A waste from thermal power stations, by high energy ball milling," *Nanoscale Research Letters*, vol. 2, no. 8, pp. 397–404, Aug. 2007, doi: 10.1007/s11671-007-9074-4.

[17] H. M. Hamada, F. Abed, Z. A. Al-Sadoon, and A. Alashkar, "Enhancing pozzolanic activity of fly ash via dry and wet milling: A comparative study for sustainable construction material enhancement," *Journal of CO2 Utilization*, vol. 83, p. 102811, May 2024, doi: 10.1016/J.JCOU.2024.102811.

[18] A. G. Patil and S. Anandhan, "Influence of planetary ball milling parameters on the mechano-chemical activation of fly ash," *Powder Technology*, vol. 281, pp. 151–158, Sep. 2015, doi: 10.1016/j.powtec.2015.04.078.

[19] P. Kanti, K. v. Sharma, C. G. Ramachandra, and A. A. Minea, "Effect of ball milling on the thermal conductivity and viscosity of Indian coal fly ash nanofluid," *Heat Transfer*, vol. 49, no. 8, pp. 4475–4490, Dec. 2020, doi: 10.1002/htj.21836.

[20] A. G. Patil and S. Anandhan, "Ball Milling of Class-F Indian Fly Ash Obtained from a Thermal Power Station," *International Journal of Energy Engineering*. 2012.

[21] R. Hamzaoui, O. Bouchenafa, S. Guessasma, N. Leklou, and A. Bouaziz, "The sequel of modified fly ashes using high energy ball milling on mechanical performance of substituted past cement," *Materials and Design*, vol. 90, pp. 29–37, 2016, doi: 10.1016/j.matdes.2015.10.109.

[22] S. Raj R, G. P. Arulraj, N. Anand, B. Kanagaraj, and E. Lubloy, "Influence of Nano-Fly Ash on mechanical properties, microstructure characteristics and sustainability analysis of Alkali Activated Concrete," *Developments in the Built Environment*, vol. 17, p. 100352, Mar. 2024, doi: 10.1016/J.DIBE.2024.100352.